Immobilized Catalysts

DOI: 10.1002/anie.200700980

Selective Formation of a Coordinatively Unsaturated Metal Complex at a Surface: A SiO_2-Immobilized, Three-Coordinate Ruthenium Catalyst for Alkene Epoxidation**

*Mizuki Tada, Rudy Coquet, Jun Yoshida, Mutsuo Kinoshita, and Yasuhiro Iwasawa**

Dedicated to Süd-Chemie on the occasion of its 150th anniversary

Immobilization of metal complexes on support surfaces is still the state of the art in the interdisciplinary field between homogeneous and heterogeneous catalysis, irrespective of long-term challenges of designing immobilized metal complexes in a controllable manner, which is currently receiving much attention in practice for a variety of catalytic chemical syntheses.[1] The potential of immobilized metal-complex catalysts strongly depends on the nature of the support surface, which can result in significant rate enhancement and novel catalytic performance that analogous homogeneous complexes do not exhibit.[1,2]

In homogeneous reactions catalyzed by metal complexes, it is suggested that a coordinatively saturated metal complex (precursor) eliminates a ligand and is converted to an active complex with an unsaturated metal center, which, because of its low stability in solution, cannot be isolated and readily undergoes aggregation leading to loss of catalytic activity.[3] On the other hand, attachment of metal complexes on the surface of oxide supports provides isolated single-site metal complexes.[1,4,5] The aim of this technique is not only the simple surface immobilization of metal complexes, but also the selective creation of unique active structures and reactivity on surfaces that are difficult to achieve in solution.[2] Here we report the synthesis of a novel three-coordinate unsaturated Ru complex on an SiO_2 surface by a new strategy and the catalytic performance of this system. A monomeric *p*-cymene-coordinated ruthenium *N*-sulfonyl-1,2-ethylenediamine complex[6] was tethered on SiO_2, and we found that exothermic reaction with O_2/isobutyraldehyde (IBA) promoted stoichiometric elimination of a *p*-cymene ligand to form an intermediate oxidant on a three-coordinate unsaturated ruthenium complex at the surface, which is active for alkene epoxidation.

The immobilized ruthenium complex was prepared in three steps (Figure 1). *N*-Sulfonyl-1,2-ethylenediamine (**A**) reacted with $[Ru_2(p\text{-cymene})_2Cl_4]$ (**B**) to form monomeric ruthenium precursor complex **C**[7] (see the Supporting Infor-

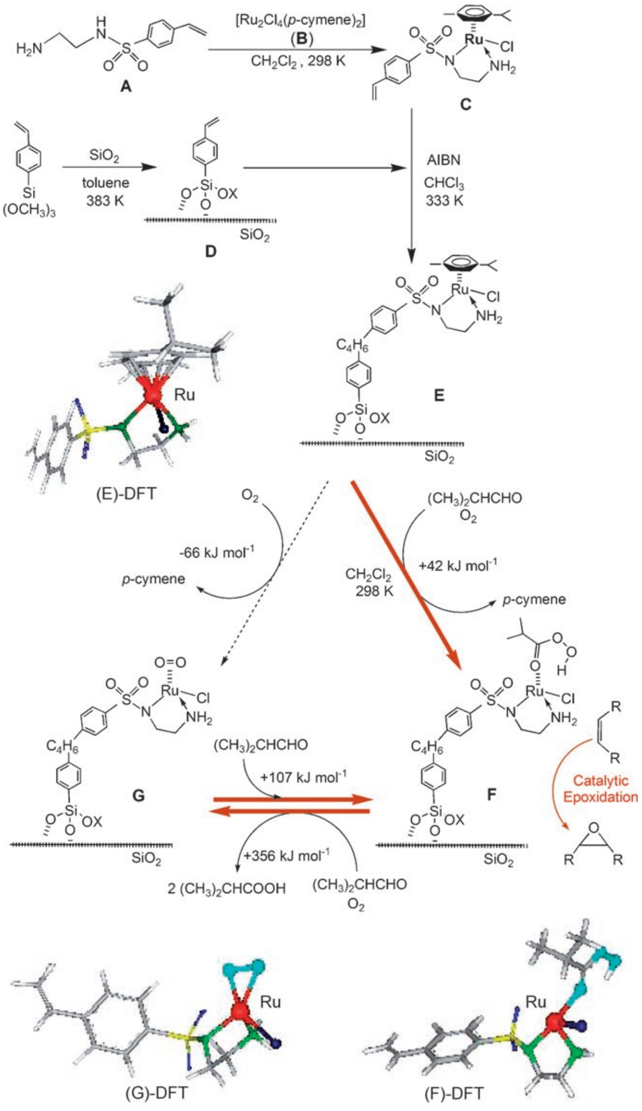

Figure 1. Preparation and structures of supported ruthenium complex **E** and single-site unsaturated active ruthenium complex **G** on SiO_2; structures calculated by hybrid DFT are also illustrated. X in **D**–**G** is Si or CH_3.

---

[*] Dr. M. Tada, Dr. R. Coquet, J. Yoshida, M. Kinoshita,
Prof. Dr. Y. Iwasawa
Department of Chemistry
Graduate School of Science
The University of Tokyo
Hongo, Bunkyo-ku, Tokyo 113-0033 (Japan)
Fax: (+81) 3-5800-6892
E-mail: iwasawa@chem.s.u-tokyo.ac.jp

[**] XAFS measurements were performed at KEK-IMSS-PF with the approval of the PF-PAC (No. 2005G209).

Supporting information for this article is available on the WWW under http://www.angewandte.org or from the author.

mation). An SiO_2 surface was modified with *p*-styryltrimethoxysilane, and ruthenium precursor complex **C** was tethered to the functionalized surface **D** by coupling with the styryl moiety to form immobilized ruthenium complex **E** with a saturated metal center bearing a *p*-cymene ligand.

The appearance of new peaks at $\delta = -62$ and -54 ppm in the ^{29}Si solid-state NMR spectrum revealed that *p*-styryltrimethoxysilane reacted with SiOH groups on the SiO_2 surface and was tethered by formation of 30% $-Si(OSi)_3$ and 70% $-Si(OSi)_2(OCH_3)$ bonds (Figure 1, **D**). The $\nu_{C=C}$ band at 1625 cm^{-1} disappeared after coupling of the styryl moieties of **C** and **D**, that is, precursor **C** was immobilized on the SiO_2 surface by reaction with **D**. The loading of the immobilized ruthenium complex was 2.7 wt% (Ru), which corresponds to 0.8 ruthenium complexes per square nanometer.

The structure of supported Ru complex **E** was characterized by X-ray photoelectron spectroscopy (XPS), diffuse-reflectance (DR) UV/Vis spectroscopy, and X-ray absorption fine structure (XAFS). In UV/Vis spectra (Figure 2), similar peaks before and after immobilization (**C** and **E**) were observed at 326 (Ru d→Ph π) and 447 nm (Cl p→Ru d). The presence of the d–π transition in the spectrum of complex **E** indicates that it has a *p*-cymene ligand, and the Ru^{2+} oxidation state and local coordination resemble those of precursor **C** (see the Supporting Information). Hence, the surface ruthenium complex **E** has the same coordination environment as precursor **C** (Figure 1).

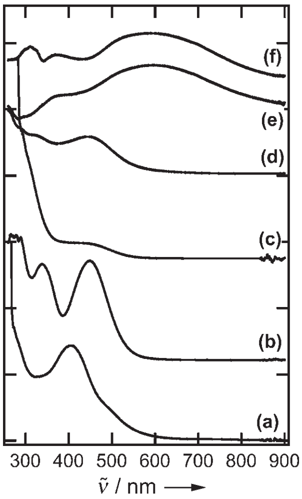

Figure 2. UV/Vis spectra of a) $RuCl_3$ in ethanol, b) **B** in CH_2Cl_2, c) **C** in CH_2Cl_2, d) supported ruthenium complex **E**, e) unsaturated Ru complex **G** activated by O_2/IBA, and f) supported Ru catalyst after 100 cycles of stilbene epoxidation. a)–c) measured in transmission mode (vertical axis: absorption); d)–f) measured in diffuse-reflectance mode (vertical axis: reflectance).

Catalytic performance in stilbene epoxidation differed greatly between the homogeneous ruthenium complexes and the supported catalyst (Table 1). $[Ru(NH_3)_6]Cl_3$ and $[Ru(bpy)Cl_2]$ (bpy = 2,2′-bipyridine) with both N-donor and chloro ligands like **E**, $[Ru_2(p\text{-cymene})_2Cl_4]$ (**B**), and $RuCl_3$ did not catalyze stilbene epoxidation with oxidants such as O_2, H_2O_2, PhIO, and O_2/IBA. The ruthenium diamine complex **C** in a homogeneous phase produced a small amount of stilbene oxide with PhIO or O_2/IBA, but the reaction stopped after a short time with formation of black precipitates. On the other hand, immobilized ruthenium complex **E** exhibited good catalytic performance with O_2/IBA: stilbene epoxidation was completed with 83–90% epoxide selectivity, while PhIO and *m*-chloroperbenzoic acid were poor oxidants with low conversion (30 and 46%, respectively) and low epoxide selectivity (16 and 41%, respectively). Epoxidation of cyclopentene, norbornene, and cyclooctene also proceeded smoothly on immobilized Ru complex **E** (Table 1).

Table 1: Catalytic activities of ruthenium catalysts for stilbene epoxidation.[a]

Catalyst	Additives	Conv. [%]	Sel. [%][b]
$[Ru(NH_3)_6]Cl_3$	IBA	0	0
$[Ru(bpy)Cl_2]$	IBA	0	0
$[Ru_2(p\text{-cymene})_2Cl_4]$ (**B**)	IBA	0	0
$[Ru_2(p\text{-cymene})_2Cl_4]$ (**B**)	IBA + ED[c]	0	0
$RuCl_3$	IBA	0	0
$RuCl_3$	IBA + ED[c]	0	0
complex **C**	none	0	0
complex **C**	H_2O_2	0	0
complex **C**	PhIO	5	22
complex **C**	IBA[d]	10	71
complex **C**	IBA + SiO_2[e]	9	66
supported catalyst **E**	none	0	0
supported catalyst **E**	H_2O_2	0	0
supported catalyst **E**	PhIO	30	16
supported catalyst **E**	CPBA[f]	46	41
supported catalyst **E**	IBA[g]	100	83
supported catalyst **E**	IBA[h]	100	90
supported catalyst **E**	IBA[i]	86	82
supported catalyst **E**	IBA[j]	100	74
supported catalyst **E**	IBA[k]	98	81

[a] CH_2Cl_2 (5 mL), 298 K, 101.3 kPa O_2, Ru (0.01 mmol), Ru/stilbene/additives = 1:50:50, 72 h. [b] (produced epoxide [mol]/consumed stilbene [mol]) × 100. [c] ED = ethylenediamine, 0.01 mmol. [d] 24 h. [e] SiO_2 (40 mg) was added. [f] *m*-chloroperbenzoic acid, 48 h. [g] 4 h. [h] Ru 0.01 mmol, Ru/stilbene/IBA = 1:1000:1000, CH_2Cl_2 (12 mL). [i] Cyclopentene epoxidation, 48 h. [j] Norbornene epoxidation, 48 h. [k] Cyclooctene epoxidation, 48 h.

Interestingly, although homogeneous complex **C** and immobilized catalyst **E** showed similar color changes under the epoxidation conditions in the presence of IBA/O_2, their catalytic performances were completely different (Table 1). Immobilized ruthenium complex **E** was converted to active unsaturated complex **G** under the catalytic reaction conditions, while the homogeneous complex **C** aggregated to form precipitates, which led to loss of the activity. Addition of SiO_2 to the homogeneous phase of **C** did not alleviate the deactivation; hence, chemical grafting on the surface is the key to preventing aggregation of the active unsaturated complexes in solution.

In the presence of an excess of IBA/O_2, the nearly stoichiometric amount of *p*-cymene (89% based on Ru) detected in the reaction solution by GC indicated release of the *p*-cymene ligand, while no release of *p*-cymene occurred under N_2 atmosphere. Hybrid DFT calculations showed that immobilized ruthenium complex **E** tends to react with IBA and O_2 with elimination of the *p*-cymene ligand and a gain of 42 kJ mol^{-1} for peroxide intermediate **F** (Figure 1). When an excess of IBA and O_2 was available, peroxide **F** was transformed into unsaturated species **G** with weakly coordinated with O_2 (O=O distance: 0.130 nm), whereby two molecules of the corresponding acid were produced in an exothermic step (356 kJ mol^{-1}). Indeed, Ru K-edge EXAFS curve-fitting analysis was consistent three-coordinate unsaturated Ru species **G** with two Ru–N bonds (coordination number 2.2) with a length of 0.207 nm and an Ru–Cl bond (coordination number 1.3) with a length of 0.234 nm (see the Supporting Information).

Ruthenium 3d XPS binding energies revealed that the valence of the immobilized Ru complex increased from 2 (**E**) to 3 (**G**) on catalyst activation with O_2/IBA (Ru $3d_{5/2}$ binding energies: **C**: 281.6, **E**: 281.5, and **G**: 282.0 eV). The oxygen molecule in optimized structure **G** was negatively charged (O_2^-). A new peak appeared in the visible region of the DR UV/Vis spectrum, at 608 nm for **G** (Figure 2), which was confirmed by time-dependent hybrid DFT.

The energy of structure **G** is 66 kJ mol^{-1} higher than that of structure **E** (Figure 1), that is, *p*-cymene elimination from **E** to form **G** does not proceed with O_2 alone. *p*-Cymene elimination does not occur with IBA either. Notably, ligand elimination can proceed by taking advantage of the exothermic reaction of IBA with O_2 on the energy-gaining route **E**→**F**→**G**, whereby the reactant IBA also has a role as initiator of active-structure formation. Furthermore, unsaturated Ru complex **G** can react with IBA to reversibly form peroxide intermediate **F** with release of 107 kJ mol^{-1} (Figure 1). In the catalytic epoxidation, the amounts of stilbene oxide and isobutyric acid were equal, that is, intermediate **F** reacted selectively with stilbene, not with IBA, to produce stilbene oxide under the catalytic reaction conditions.

After 1000 cycles of stilbene epoxidation, characterization of the ruthenium complex showed retention of the three-coordinate unsaturated structure (see the Supporting Information), and unsaturated Ru complex **G** was active in the epoxidation reaction. It is noteworthy that three-coordinate ruthenium complex **G** is quite stable under the reaction conditions and also in air, in spite of its unsaturated structure. This remarkable stability and durability make immobilized catalyst **G** recyclable in catalytic reactions with retention of 100 % conversion and selectivity exceeding 80 % (see the Supporting Information). There was no decrease in the ruthenium loading of the supported catalyst and no leaching of the ruthenium complex into the solution phase after three recycling processes of stilbene epoxidation (100 catalytic cycles for each run).

Low stability of an unsaturated metal complex leading to aggregation or decomposition in solution prevents exploitation of metal-complex catalysis. Immobilization of metal complexes to isolate the unsaturated metal centers on solid surfaces is promising, not only for dramatic improvement of catalytic activity, but also for a better understanding of key issues in catalysis by unsaturated metal-complex structures. We have presented a new way to create a three-coordinate Ru complex on an SiO_2 surface which is stable in air but active for catalytic stilbene epoxidation. The unsaturated ruthenium complex cannot be produced by ligand elimination and exchange, but can be generated in conjunction with an exothermic reaction in the coordination sphere.

Experimental Section

N-Sulfonyl-1,2-ethylenediamine (**A**) and ruthenium precursor complex **C** were synthesized by literature methods[7] (see the Supporting Information). SiO_2 (Aerosil 200, Degussa) was calcined at 773 K for 2 h and refluxed in a solution of *p*-styryltrimethoxysilane in anhydrous toluene at 383 K for 18 h under N_2. The SiO_2 was subjected to Soxhlet extraction and then dried under vacuum. The amount of grafted *p*-styryl moieties was 1 nm^{-2}. The ruthenium precursor **C** (135 mg) was treated with **D** (0.67 g) in anhydrous $CHCl_3$ (10 mL) in the presence of 2,2′-azobis(isobutyronitrile) (AIBN, 1.1 mg) and then refluxed at 333 K for 24 h under N_2 atmosphere. The obtained ruthenium complex on SiO_2, **E**, was subjected to Soxhlet extraction and dried under vacuum.

Supported ruthenium complex **E** was activated in CH_2Cl_2 with an equivalent amount of IBA relative to Ru under an atmospheric pressure of O_2. After a few minutes, activation was complete, the reaction solution was filtered, and the obtained sample was dried under vacuum. These catalysts were characterized by solid-state NMR (Chemagnetics CMX-300), FTIR (JASCO FT/IR-4200ST), XPS (Rigaku XPS-7000), DR UV/Vis (JASCO V-550-DS), and XAFS (KEK-PF, BL-10B and NW10A).

Hybrid DFT calculations were performed with the Gaussian 03 package,[8] and time-dependent DFT was applied to calculate UV/Vis transitions. The PBE0 hybrid functional[9] was employed together with the DGDZVP[10] basis set. PBE0 is a nonempirical hybrid GGA functional and combines the lack of any adjustable parameter with remarkable results for a number of physicochemical observables.[11] Choosing DGDZVP allows the use of a relatively large and accurate basis set for all atomic species including Ru, without the need for any pseudopotential. The UV/Vis spectra were generated by using the SWizard program, revision 4.2[12] with the Gaussian model, and the half-bandwidths were taken to be equal to 3000 cm^{-1}. The VModes program, rev. A 7.2f was employed to calculate the contribution percentage from selected atomic orbitals to molecular orbitals and thus to assign UV/Vis transitions.

Alkene epoxidation was performed at 298 K in CH_2Cl_2 under an atmospheric pressure of O_2. The reactants and products were analyzed by GC (Shimadzu GC-14A) and GC-MS (Shimadzu GC-2010) at appropriate intervals. The supported catalyst was recycled by filtration and addition of the reactants and IBA. The loading of the ruthenium complex on the surface was confirmed by XRF (Seiko SEA-2120L).

Received: March 6, 2007
Revised: April 25, 2007

Keywords: epoxidation · heterogeneous catalysis · immobilization · ruthenium · surface chemistry

---

[1] a) J. M. Thomas, R. Raja, D. W. Lewis, *Angew. Chem.* **2005**, *117*, 6614; *Angew. Chem. Int. Ed.* **2005**, *44*, 6456; b) M. Tada, Y. Iwasawa, *Chem. Commun.* **2006**, 2833; c) J. M. Notestein, A. Katz, *Chem. Eur. J.* **2006**, *12*, 3954; d) P. McMorn, G. J. Hutchings, *Chem. Soc. Rev.* **2004**, *33*, 108; e) R. A. Sheldon, M. Wallau, I. W. C. E. Arends, U. Schuchardt, *Acc. Chem. Res.* **1998**, *31*, 485; f) A. Corma, H. Garcia, *Adv. Synth. Catal.* **2006**, *348*, 1391; g) C. Copéret, J. M. Basset, *Adv. Synth. Catal.* **2007**, *349*,

78; h) J. C. Fierro-Gonzalez, S. Kuba, Y. L. Hao, B. C. Gates, *J. Phys. Chem. B* **2006**, *110*, 13326.

[2] a) M. Tada, T. Taniike, L. M. Kantam, Y. Iwasawa, *Chem. Commun.* **2004**, 2542; b) M. Ramin, J. D. Grunwaldt, A. Baiker, *J. Catal.* **2005**, *234*, 256; c) K. Yamaguchi, C. Yoshida, S. Uchida, N. Mizuno, *J. Am. Chem. Soc.* **2005**, *127*, 530; d) C. Bianchini, V. Dal Santo, A. Meli, S. Moneti, M. Moreno, W. Oberhauser, R. Psaro, L. Sordelli, F. Vizza, *J. Catal.* **2003**, *213*, 47.

[3] a) M. Yamakawa, H. Ito, R. Noyori, *J. Am. Chem. Soc.* **2000**, *122*, 1466; b) F. Simal, L. Wlodarczak, A. Demonceau, A. F. Noels, *Eur. J. Org. Chem.* **2001**, 2689.

[4] a) J. Joubert, F. Delbecq, P. Sautet, E. Le Roux, M. Taoufik, C. Thieuleux, F. Blanc, C. Coperet, J. Thivolle-Cazat, J. M. Basset, *J. Am. Chem. Soc.* **2006**, *128*, 9157; b) P. Barbaro, C. Bianchini, V. Dal Santo, A. Meli, S. Moneti, R. Psaro, A. Scaffidi, L. Sordelli, F. Vizza, *J. Am. Chem. Soc.* **2006**, *128*, 7065; c) C. A. Kruithof, M. A. Casado, G. Guillena, M. R. Egmond, A. van der Kerk-van Hoof, A. J. R. Heck, R. J. M. K. Gebbink, G. van Koten, *Chem. Eur. J.* **2005**, *11*, 6869.

[5] a) M. Tada, T. Sasaki, Y. Iwasawa, *J. Phys. Chem. B* **2004**, *108*, 2918.

[6] K.-J. Haak, S. Hashiguchi, A. Fujii, T. Ikariya, R. Noyori, *Angew. Chem.* **1997**, *109*, 297; *Angew. Chem.* **1997**, *36*, 285.

[7] a) H. Kamogawa, A. Kanazawa, M. Kadoya, T. Naito, M. Nakasawa, *Bull. Chem. Soc. Jpn.* **1983**, *56*, 762; b) K. Polborn, K. Severin, *Chem. Eur. J.* **2000**, *6*, 4604.

[8] Gaussian 03, Revision B.05, M. J. Frisch et al., Gaussian, Inc., Wallingford CT, **2004**.

[9] J. P. Perdew, K. Burke, M. Ernzerhof, *Phys. Rev. Lett.* **1996**, *77*, 3865.

[10] C. Sosa, J. Andzelm, B. C. Elkin, E. Wimmer, K. D. Dobbs, D. A. Dixon, *J. Phys. Chem.* **1992**, *96*, 6630.

[11] a) C. Adamo, G. E. Scuseria, V. Barone, *J. Chem. Phys.* **1999**, *111*, 2889; b) G. Scalmani, J. L. Bredas, V. Barone, *J. Chem. Phys.* **2000**, *112*, 1178.

[12] S. I. Gorelsky, *SWizard program*, York University, Toronto, Canada, **1998**.